LBL-27629
Preprint

Lawrence Berkeley Laboratory
UNIVERSITY OF CALIFORNIA

Materials & Chemical Sciences Division

Submitted to Journal of Chemical Physics

The Translational Energy Dependence of the $F + C_2H_4 \rightarrow H + C_2H_3F$ Reaction Cross Section near Threshold

G.N. Robinson, R.E. Continetti, and Y.T. Lee

August 1989

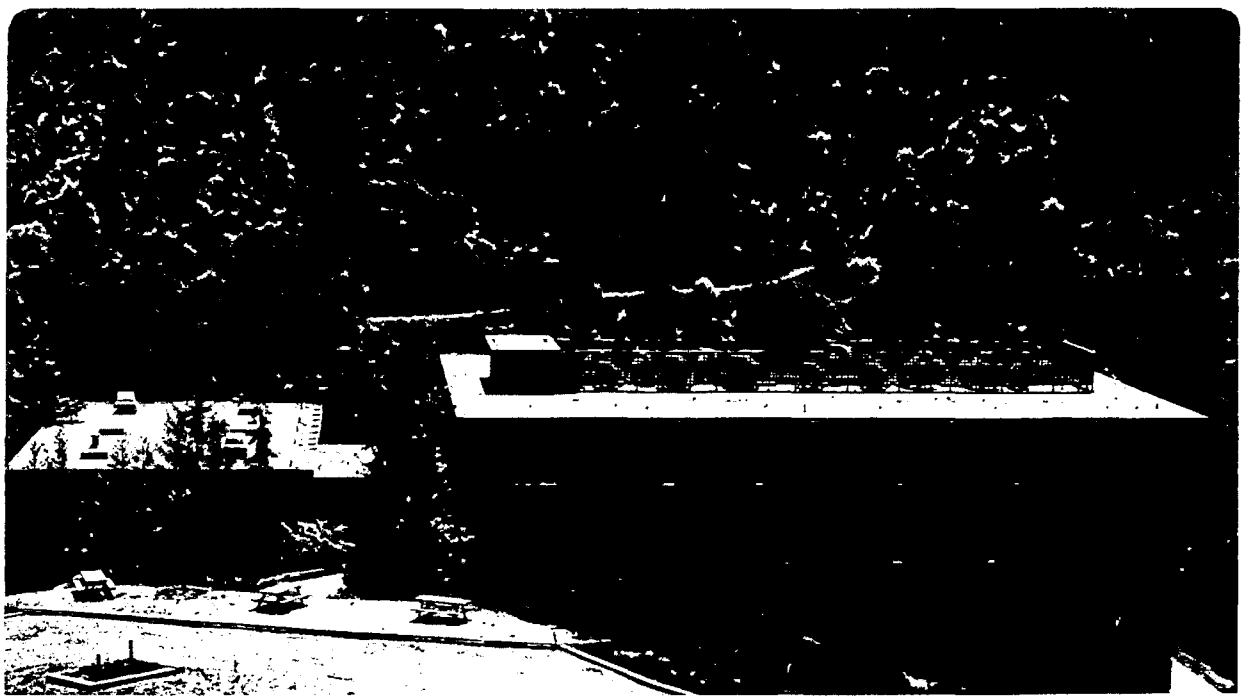

LOAN COPY
Circulates
for 2 weeks
Bldg. 50 Library.
LBL-27629
Copy 2

Prepared for the U.S. Department of Energy under Contract Number DE-AC03-76SF00098.

DISCLAIMER

This document was prepared as an account of work sponsored by the United States Government. While this document is believed to contain correct information, neither the United States Government nor any agency thereof, nor the Regents of the University of California, nor any of their employees, makes any warranty, express or implied, or assumes any legal responsibility for the accuracy, completeness, or usefulness of any information, apparatus, product, or process disclosed, or represents that its use would not infringe privately owned rights. Reference herein to any specific commercial product, process, or service by its trade name, trademark, manufacturer, or otherwise, does not necessarily constitute or imply its endorsement, recommendation, or favoring by the United States Government or any agency thereof, or the Regents of the University of California. The views and opinions of authors expressed herein do not necessarily state or reflect those of the United States Government or any agency thereof or the Regents of the University of California.

The Translational Energy Dependence of the $F + C_2H_4 \rightarrow H + C_2H_3F$ Reaction Cross Section near Threshold

Gary N. Robinson*, Robert E. Continetti, and Yuan T. Lee

Materials and Chemical Sciences Division,
Lawrence Berkeley Laboratory and Department of Chemistry,
University of California, Berkeley, CA 94720

* Present address: Department of Chemistry, Princeton University, Princeton, NJ

ABSTRACT

We have carried out crossed molecular beam studies of the substitution reaction $F + C_2H_4 \rightarrow H + C_2H_3F$ in the collision energy range 0.8 - 2.5 kcal/mol using a velocity selected F atom beam. The relative substitution cross section is found to decrease with increasing collision energy indicating that if there is a potential energy barrier to F atom addition to C_2H_4 it is much less than 0.8 kcal/mol and that the transition state for addition occurs early along the reaction coordinate. These results agree well with ab initio calculations. Although the product translational energy distributions are similar to those obtained from earlier work at higher collision energies, the C_2H_3F angular distributions suggest that a wider range of reactant approach geometries lead to products at lower energies.

I. INTRODUCTION

An understanding of potential energy barriers is central to the field of chemical kinetics. Although activation energies can be extracted from the temperature dependence of reaction rates, these are phenomenological quantities that cannot always be directly correlated with the mechanical barrier on the potential energy surface (PES). The most direct way to probe such a barrier is to measure the translational energy dependence of the reaction cross section, or the excitation function. In an effort to learn more about the potential energy surfaces for atom-molecule addition reactions, we have studied the excitation function of the reaction $F + C_2H_4 \rightarrow H + C_2H_3F$ at six collision energies in the range 0.8 - 2.5 kcal/mol using the crossed molecular beams method. The energetics of this reaction are outlined in Fig. 1.

There have been few kinetic studies of F + alkene substitution reactions owing largely to the experimental difficulties caused by the high reactivity of fluorine atoms. Notable, however, are experiments by Wolfgang on $^{18}F + C_2H_4$ [1] and more recent work by Rowland and coworkers on the relative reactivity of ^{18}F with various substrates [2]. Pukhal'skaya <u>et al.</u> [3] have measured the rate of reaction of $F + C_2H_4$ to give both substitution (C_2H_3F) and abstraction (HF) products by monitoring the quenching of HF chemiluminescence from the reaction $F + H_2$ caused by the reaction $F + C_2H_4$.

Earlier crossed molecular beam studies of the title reaction [4] yielded center-of-mass (CM) frame C_2H_3F angular distributions that were forward-backward symmetric, indicating that the reaction proceeds through a collision complex which decomposes on a time scale longer than its rotational period. In addition, the CM angular distributions peaked slightly at θ=90°, suggesting that the F atom adds roughly perpendicular to the plane of the C_2H_4 double bond and that the H atom is ejected parallel to the total angular momentum vector (see Section III). The product translational energy distribution, P(E'), could not be reproduced by a statistical model that assumes that energy is completely randomized in the intermediate complex and that the P(E') reflects the distribution of vibration-rotation states along the reaction coordinate at the exit-channel transition state (TS). From chemiluminescence experiments, McDonald and co-workers [5] likewise concluded that the internal state distribution of the C_2H_3F product reflects a non-statistical partitioning of energy in the collision complex.

Marcus [6,7] has pointed out that for a "tight" transition state such as H-C_2H_3F, where there are no free internal rotations, exit channel interactions between the departing fragments will tend to shift the product translational energy distribution to higher energies, complicating any comparison of the experimental and RRKM P(E') distributions. Classical trajectory calculations by Hase and Bhalla [8] on a semi-empirical F + C_2H_4 PES fitted to SCF saddle point energies for

$F-C_2H_4$ [9] and $H-C_2H_4$ [10] indicate that the relative product translational energy distribution is indeed statistical at the exit channel saddle point but that it becomes skewed to higher energies as the products descend the 5 - 6 kcal/mol barrier to H atom elimination from C_2H_3F. Ref. 4c shows, however, that the form of the P(E') changes little when the excess energy at the exit transition state is about five times larger than this barrier, suggesting that the P(E') really does reflect non-statistical energy redistribution in the collision complex.

The reaction $F + C_2H_4 \rightarrow [C_2H_4F]^*$ is representative of a broad class of radical-alkene addition reactions. The activation energies for these reactions are typically low (0 - 10 kcal/mol) [11,12,13]. There has, however, been considerable discussion in the literature about the factors that determine the magnitudes of these activation energies. Using a three-electron, three-center valence bond model, Salem and co-workers [14] conclude that the degree of ionic character in the incipient radical-alkene bond determines the magnitude of the activation energy. Essentially, including polar resonance structures of the adduct radical lowers the calculated activation energy to addition. Thus halogen atom addition to ethylene is expected to have a lower activation energy than methyl radical or hydrogen atom addition and this is indeed the case (Cl: 0 kcal/mol; H: 2.8 kcal/mol; CH_3: 7.7 kcal/mol) [12]. Alternatively, for many reactions the activation energy is roughly proportional to the difference between the ionization

potential of the alkene and the electron affinity of the incoming atom [15]. Here again, the more polar the new bond, the lower the activation energy. From a series of experiments on radical addition reactions, Tedder and Walton [16] likewise find an inverse correlation between the polarity of the incipient bond and the activation energy. These activation energies also correlate well with Hückel localization energies [16,17], the π-electron energy that is lost upon forming the adduct, although when comparing the reactivities of different radicals with the same substrate the localization energy is not a particularly useful quantity.

Ab initio quantum chemical calculations offer more detailed insights into the potential energy surfaces for addition reactions. Using unrestricted Hartree-Fock (UHF) theory, Kato and Morokuma [10] have found that the largest contribution to the 5 - 6 kcal/mol barrier to H atom addition to C_2H_3F (the reverse of the reaction here under study) comes from the deformation energy, or the energy required to distort the ethylene to its transition state configuration. Schlegel et al. [18] have calculated the barrier to F atom addition to ethylene to be 3.0 kcal/mol at the HF level using an optimized transition structure from a second-order Moller-Plesset (MP) perturbation calculation in which the C-F bond length is 2.0 Å, the F-C-C angle is 94°, and the ethylene moiety is essentially undistorted [19]. The C-C-F bending frequencies that they calculate for this structure (242 and 405 cm^{-1}) suggest a "tight" transition

state. Accounting for electron correlation through third and fourth-order MP theory reduces the barrier to less than 2 kcal/mol and causes the F-C_2H_4 transition structure to become even more reactant-like. UHF calculations by Clark et al. [9] indicate that, although the computed saddle point geometry of the adduct corresponds to an early, or reactant-like, TS, the electron density is characteristic of a more product-like TS. They calculate an activation energy of 3.1 kcal/mol for addition. By eliminating spin contamination from their UHF wave functions, Sosa and Schlegel [20] have recently obtained a barrier height of -0.9 ± 0.3 kcal/mol for OH + $C_2H_4 \rightarrow C_2H_4OH$, which yields an activation energy that is in close agreement with experiment. They also conclude [21] that F atom addition to C_2H_4 will have no barrier. Most recently Engels and Peyerimhoff [22] have carried out a full CI calculation of the F + $C_2H_4 \rightarrow C_2H_4F$ potential along the reaction coordinate in which they find no barrier to either asymmetric or symmetric F atom addition, i.e., addition to either a carbon atom or across the double bond. However, the energy of the bridged fluoroethyl radical is computed to be 27 kcal/mol higher than that of the asymmetric radical. As we will show, our results are in close agreement with these higher level quantum mechanical calculations.

II. EXPERIMENTAL

The experimental apparatus has been described elsewhere [23,24]. Ref. 24 contains a detailed description of the F atom source and of the pumping configuration for both sources and for the detector. Briefly, a doubly differentially pumped, velocity selected F atom beam was crossed with a singly differentially pumped, supersonic ethylene beam at 90° in a reaction chamber held at about 10^{-7} torr. Product C_2H_3F signal, m/e=46, was measured with a mass spectrometric detector that rotates in the plane of the two beams.

The primary beam was produced by velocity selecting an effusive F atom beam formed by thermally dissociating pure F_2 (Matheson) in a resistively heated nickel oven. The oven temperature was approximately 650°C. The six disk velocity selector gave a fwhm velocity spread of 11% which was independent of the wheel frequency. The angular divergence of the F beam was ≈2°.

The supersonic ethylene beam was produced by expanding 500 torr of ultra-high purity ethylene (Matheson) or 20% ethylene in helium through a 0.21 mm diameter nozzle. The source consisted of a platinum electron microscope aperture brazed onto a copper tube. The nozzle was held at a distance of 1.0 cm from a 0.81 mm aperture stainless steel skimmer. A coaxial heater and a liquid nitrogen contact allowed us to vary the temperature of the source.

Table 1 lists the experimental beam conditions. Changing the velocity selector frequency and/or seeding or cooling the ethylene beam enabled us to vary the collision energy, E_c. Experiments were carried out at six nominal collision energies: 0.8, 1.1, 1.4, 1.9, 2.0, and 2.5 kcal/mol. The fwhm spread in collision energy was ≈20%.

Product angular distributions were obtained by modulating the F atom beam with a 150 Hz tuning fork chopper. Counting times ranged from 2-17 minutes per angle. Time-of-flight (TOF) spectra of the reactive product were measured using the cross-correlation method [23b] near the center-of-mass angle for four of the six collision energies. A 255-channel multi-channel scaler connected to a LSI/11 minicomputer controlled the data acquisition. A Cu-Be wheel, photoetched with a 255 element pseudo-random sequence of open and closed slots, was spun at 436 Hz giving 9 μsec/ channel resolution in the TOF spectra. The flight path from the chopping wheel to the ionizer was 30.4 cm. Counting times were from 1-4 hours per angle. The velocity distributions of both reactant beams were measured by spinning a stainless steel wheel with four equally spaced slots at 300 Hz.

III. RESULTS AND ANALYSIS

The product angular distributions are plotted in Figs. 3 - 8; low level elastic scattering background from impurities has been subtracted. More structure is evident in these distributions than in those of the earlier studies as a result of the improved product velocity and angular resolution of the present apparatus and the narrower velocity spread of the fluorine beam. The bimodality of the TOF spectra (Fig. 9) indicates that the product recoil energy distribution peaks away from zero (Fig. 2).

The product angular distributions and TOF spectra were fit using a forward convolution program that starts with a separable form for the CM frame product flux distribution [25], $I_{CM}(\theta,E') = T(\theta)P(E')$, and generates LAB frame angular distributions and TOF spectra averaged over the spread in relative velocities and the apparatus resolution. $T(\theta)$, the CM frame product angular distribution, was initially taken to be a sum of Legendre polynomials whose coefficients were varied to optimize the fit. A point-form was used for the CM frame product translational energy distribution, $P(E')$. The fits were refined by altering sections of $T(\theta)$ and $P(E')$.

The $T(\theta)$ distributions (Fig. 10) are largely symmetric about $\theta=90°$ confirming the earlier findings [4] that the reaction proceeds via a long-lived collision complex. However, unlike the earlier studies, in which the CM angular distribu-

tions rise monotonically from 0° to 90° (with T(0°)/T(90°) ≃ 0.7 at E_c=2.0 kcal/mol), we observe forward-backward as well as a sideways peaking at some energies. Presented in Figs. 3 - 8 are fits to the LAB angular distributions using different CM frame angular distributions. The E_c=1.9, 2.0, and 2.5 kcal/mol LAB distributions are fit adequately by T(θ) distributions having a single maximum at θ=90°, but the fits to the E_c=1.9 and 2.0 kcal/mol data are improved a bit by including smaller peaks at 0° and 180° (Fig. 10; a,b). A slight excess of forward scattering improves the fit to the E_c=1.9 kcal/mol distribution.

The LAB angular distribution at E_c=1.4 kcal/mol has a pronounced dip at θ≈65°. This dip can be fit only if T(θ) has a local minimum at θ≈150°. In fact, the fit to the forward portion of the LAB angular distribution is rather insensitive to the form of T(θ) from θ=0°-90°. Forcing T(θ) to be approximately forward-backward symmetric gives distributions c(i) and c(ii) in Fig. 10, which have maxima at 0° and 180° and a broad peak ≈90°. These distributions are still slightly asymmetric, the valley at 150° being wider, and in the case of c(ii), deeper than the valley at 30°. In deriving distribution c(ii), an effort was made to keep the ratio T(0°)/T(90°) as small as possible. A T(θ) similar to that used in ref. 4 which has a single maximum at 90° does not fit the the backward portion of the LAB distribution well. T(θ) distributions b(i) and b(ii) also yield poor fits, giving too much intensity near θ_{CM}.

Although the signal-to-noise ratio is worse at E_c=1.1 kcal/mol, the LAB angular distribution at this energy also shows a backward dip. The data can be fit with CM distributions c(i) and c(ii). Again, the fit to the forward part of the LAB angular distribution is insensitive to the form of $T(\theta)$ from 0°-90° and a sideways peaked distribution does not fit the backward part of the LAB distribution. The E_c=0.8 kcal/mol data is too noisy to be fit with certainty; an adequate fit is obtained with an isotropic $T(\theta)$ although their is a hint of a peak near θ_{CM}.

Changing $T(\theta)$ at E_c=1.4 and 1.1 kcal/mol as described above barely changed the calculated TOF spectra. In retrospect, it would have been wise to measure product TOF spectra at more than one angle but at the time of these experiments we did not suspect that the CM angular distributions would be different from those obtained earlier.

Two different models have been proposed to explain the sideways peaked angular distributions observed in the earlier crossed beam studies of this reaction. Lee and co-workers have argued [4] that if the F atom adds roughly perpendicular to the plane of C_2H_4 molecule and if the rotational angular momentum of the C_2H_4 reagent is small, then the heavy atoms (C-C-F) will rotate in a plane containing the relative velocity vector, **v**, and perpendicular to the orbital angular momentum vector, **L**. Since the H atom will be perpendicular to the C-C-F plane (and hence to **v**) in the exit channel transition state, the products

will scatter sideways and parallel or anti-parallel to **L**. However, this sort of scattering occurs only because **L'** << **L**, which is to say that the rotational angular momentum vector of the C_2H_3F product, **j'**, is oriented parallel to **L** **[26]**.

McClelland and Herschbach [27] have pointed out that, being a nearly prolate top [28], the fluoroethyl radical will rotate predominantly about its A-axis (the axis corresponding to it smallest moment of inertia) while this axis precesses about the total angular momentum vector, **J**. Averaging over the relative orientations of **A**, **J**, **v**, and **v'**, they arrived at a CM angular distribution that is sideways peaked. In calculating these cylindrical averages, however, they assume that there is a steric preference for F atom attack perpendicular to the double bond and that the H atom is ejected perpendicular to the C-C-F plane.

The rotation of the complex about its **A**-axis is certainly important to consider. But the question is which type of rotation dominates in the complex? When the heavy atoms (C-C-F) rotate nearly in a plane (with total angular momentum vector perpendicular to that plane), scattering at 0° and 180° occurs only when some fraction of the C_2H_4F complexes decompose with their C_β-H^* bond (the bond that is breaking) lying in the <u>initial</u> C-C-F plane. If the C_β-H^* bond is perpendicular to the C-C-F framework, it can lie in the initial C-C-F plane only if the radical rotates about its **A**-axis. Our data, which show a change in the product angular distribution from Fig. 10(a) to

10(b) to 10(c) as the collision energy is decreased from 2.5 kcal/mol to 1.1 kcal/mol, might therefore reflect the transition from the dominance of end-over-end C-C-F rotation to the increased importance of rotation about the C-C bond axis. In particular, as the collision energy is lowered and long range attractive forces between the atom and molecule become dominant (see next section), collisions involving F atoms striking slightly away from, but near the mid-point of, the C=C bond may increasingly lead to complex formation. The total angular momentum vector of such a complex will lie closer to the original C-C axis; the C_β-H^* bond will rotate, to a greater extent, perpendicular to the total angular momentum vector and the product angular distribution will display forward-backward peaking. If the angular momentum of this type of motion in a complex is comparable to that of the end-over-end C-C-F rotational motion (which is responsible for the sideways scattering), we may observe peaks in the CM angular distribution at 0°, 90°, and 180°. It should be noted again that the CI calculations Engels and Peyerimhoff indicate that there is no barrier to symmetric addition of F to C_2H_4 [22]. Also, by analogy with the HF-C_2H_4 [29] and OH-C_2H_4 [20] van der Waals complexes, a loose F-C_2H_4 complex is likely to have a non-planar T-shaped structure.

The rotational angular momentum, **j**, of the ethylene molecule will also contribute to the total angular momentum of the C_2H_4F complex and therefore affect the symmetry of $T(\theta)$.

However, it will constitute only a small fraction of **J**. Taking the rotational temperature of the ethylene molecules in the beam to be ≈30 K, we calculate the peak of the rotational state distribution to be **j** = 3 $\hbar$. From their classical trajectory calculations, Hase and Bhalla concluded that the maximum impact parameter for the F + C_2H_4 addition reaction is 2.5 Å [8], but, not knowing the opacity function for this reaction, it is not possible to calculate **L** accurately. Assuming an average impact parameter of 2.0 Å, **L** ≈ 50 $\hbar$ at E_c=2.5 kcal/mol and 30 $\hbar$ at 0.8 kcal/mol. So, at most, **j** ≈ (0.1) **J**. Molecular rotations might be more relaxed in the seeded C_2H_4 beam (E_c=2.5 and 2.0 kcal/mol) but the best fit CM angular distributions for the 1.9 kcal/mol data, obtained with a neat C_2H_4 beam, are rather similar to those at the two highest energies. In any case, the rotational angular momentum of the ethylene molecule would be expected to make T(θ) more, rather than less, isotropic.

It should be noted that the C_2H_3F product scatters over a wider range of LAB angles at the lower collision energies as a result of the different kinematics. For instance, the distances between the peaks of the forward and backward lobes of the angular distributions are about 24°, 25°, 18°, and 16° at E_c=1.1, 1.4, 2.0, and 2.5 kcal/mol respectively. Thus, the lower energy angular distributions might actually afford a more detailed insight into the dynamics of this reaction. Hase [30] is currently carrying out classical trajectory calculations on this reaction at low collision energies to see what effect

angular momentum partitioning has on the differential cross section.

The calculated P(E') distributions (Fig. 11) are in general agreement with those of ref. 4 in that approximately 50% of the available energy is channeled into translation (Table 2). The data at different collision energies could be fit using P(E') distributions having similar forms. The fits are most sensitive to the peak values and thresholds of the translational energy distributions. The threshold of the E_c=2.5 kcal/mol P(E') is uncharacteristically high. This is undoubtedly due to the fact that, since there is no TOF data at this energy, the determination of the P(E') is based solely on the product angular distribution.

Although it was found in the earlier scattering studies that an exoergicity of 13 kcal/mol was necessary to fit the data, the present fits are not very sensitive to the cutoff energies of the P(E'). Accordingly, we take ΔH°= -11 kcal/mol, which is the difference between the product and reactant heats of formation at 300 K [15]. Adding a tail of up to 2 kcal/mol additional energy to the P(E') did not affect the calculated angular and TOF distributions.

Since the ethylene beam was cooled to -100°C in order to reach the two lowest collision energies, small amounts of clusters of various sizes were present in the beam. Fluorine atoms condense on these clusters and the resulting complexes have the velocities of the centers-of-mass [31]. Since the

center-of-mass angle moves progressively closer to the ethylene beam as the cluster size increases, fragmentation of these complexes in the electron bombardment ionizer will give rise to a large nonreactive m/e=46 signal near the ethylene beam. This spurious signal was neglected in the fits of the E_c=0.8 and 1.2 kcal/mol product angular distributions. Also, in order to minimize detector background, no data was ever collected at angles closer than 7° to the ethylene beam.

Relative cross sections, S_r, were obtained by integrating the CM frame product flux (Table 2; Fig. 12):

$$S_r = 2\pi \int_0^\infty \int_0^\pi P(E')T(\theta) \sin\theta \, dE' d\theta \ .$$

Since the product angular distributions were measured over a period of several weeks, fluctuations in the F oven temperature and consequently in the F beam intensity unavoidably occurred. Also, because the collision energy was varied by lowering the velocity selector frequency and cooling or seeding the ethylene beam, the intensities of both beams varied considerably over the energy range studied. For example, at a velocity selector frequency of 500 Hz the most probable F atom velocity is 8.7 x 10^4 cm/sec. This velocity is near the peak of the Maxwell-Boltzmann velocity distribution at 650°C. From 500 Hz to 250 Hz (8.7 to 4.3 x 10^4 cm/sec) the F atom number density drops by a factor of 21. Likewise, on cooling the ethylene beam to -100°C the observed m/e=28 number density drops as a result of cluster formation. Seeding 20% ethylene in helium leads to a slight increase in the monomer number density. Thus, in order

to compare the integrated product flux at different collision energies, one day was spent measuring beam intensities and product signal at two laboratory angles at each collision energy for which a complete product angular distribution was already measured. The signals at both angles were divided by the corresponding signals from the complete angular distributions giving two normalization factors. The computed relative cross sections were scaled using the average of these two normalization factors. To account for changes in reactant flux, the cross sections were further scaled by a reactant flux factor, $n_F n_{C_2H_4} v_{rel}$, where n_i is the number density of the i-th beam and v_{rel} is the relative velocity.

Relative reactant number densities were determined by directly measuring reactant count rates. Since the F/F_2 ratio changes with velocity (because the two species have different Maxwell-Boltzmann velocity distributions), one needs to know the percentage of F_2 that fragments in the ionizer to give m/e=19. We had hoped to determine the extent of fragmentation of F_2 by comparing the experimental velocity distributions for F and F_2 with the Maxwell-Boltzmann distributions. However, since the F atom beam was not truly effusive ($\Delta v/v \approx 30\%$ (fwhm)), no such comparison was possible.

Earlier measurements in our laboratory on the dissociative ionization of F_2 from a 650°C supersonic nozzle yielded $F^+/F_2^+ = 0.47$ [32]. However, it can be seen in Fig. 13 that this value for F^+/F_2^+ causes the excitation function to behave

non-monotonically. A more reasonable value is $F^+/F_2^+ = 0.20$ since it causes the slope of the excitation function between E_c=1.9 and 2.0 kcal/mol to have a value less than that between 1.4 and 1.9 kcal/mol and greater than that between 2.0 and 2.5 kcal/mol (Fig. 13). Setting $F^+/F_2^+ = 0.27$ makes $S_r(1.9) = S_r(2.0)$.

The uncertainties associated with the reactant flux scaling factors are neglected since the statistical errors in the n_i values are very small and the relative cross section does not change considerably over the spread in v_{rel}. The largest uncertainty in the relative cross section, represented by the error bars in Fig. 12, arises from the first scaling factor and reflects the statistical noise in the data. It should also be noted that weighting the relative velocities used in the analysis by the experimental excitation function (Fig. 12) had no effect on the E_c=1.4 kcal/mol fit. This is to be expected since the spread in collision energy is a small fraction of the total energy available to the products.

The decrease in the relative substitution cross section with increasing collision energy indicates that the barrier to F atom addition is likely nil, but in any case must be less than 0.8 kcal/mol. Since $T(\theta)$ is weighted by $\sin\theta$ in calculating S_r, S_r will be most sensitive to the form of $T(\theta)$ near θ=90°. For the E_c=1.9 kcal/mol data, however, a 10% change in $T(\theta)$ at θ=90° caused less than a 1% deviation in S_r. At E_c=0.8 kcal/mol, an isotropic $T(\theta)$ yields a value of S_r that is only 2% larger than

the value obtained using distribution d(i). Likewise, changing the position of the threshold or the peak of P(E') enough to perceptibly worsen the fit changes S_r by only 3%. However, the lack of data at $\theta > 82°$ for four of the six collision energies (and especially at E_c=0.8 kcal/mol) necessarily introduces some error in S_r.

Raising the ethylene beam nozzle temperature from -100° to 30°C changes the fraction of molecules that are in their ground vibrational states negligibly. The largest change (≈2%) will occur in the population of ν_{10}, the CH_2 rocking mode (843 cm^{-1} [33]). Hase et al. have run classical trajectories on semi-empirical potential energy surfaces to study the effect of vibrational excitation of C_2H_4 on the $H + C_2H_4 \rightarrow C_2H_5$ reaction cross section [34]. They find that placing up to 2 quanta in ν_2 (1655 cm^{-1}; C-C stretch), ν_7 (969 cm^{-1}; CH_2 wag), or ν_8 (959 cm^{-1}; CH_2 wag) has little effect on the addition cross section.

IV. DISCUSSION

In attempting to explain the decrease of S_r with increasing collision energy, let us first consider the predictions of statistical reaction rate theory. Assuming that the probability of adduct formation is independent of collision energy in the range studied, the observed excitation function will reflect the probability of unimolecular decay of the energized fluoroethyl radical to products relative to the reverse reaction forming

reactants or to other energetically accessible products. Rate constants for these decay pathways, k_i, can be calculated as a function of energy from RRKM theory and the branching ratio,

$$S^p_{RRKM} = k_p / \sum_i k_i,$$

where p represents the H atom elimination channel, can then be compared to the observed excitation function. Each rate constant reflects the state density at the transition state for a given pathway so, for an exoergic reaction, the above ratio is expected to decrease on increasing the collision energy since the state density at the reactant ($F-C_2H_4$) transition state increases more rapidly with energy in the threshold region than the state density at the product ($H-C_2H_3F$) transition state.

In addition to atomic elimination, we must, however, consider the possibility of exothermic 3- and 4-center HF elimination:

$$F + C_2H_4 \rightarrow C_2H_3 + HF \ (v=0-2), \quad \Delta H^\circ_0 \simeq -23 \text{ kcal/mol}.$$

In the crossed beam study of the reaction $F + C_2D_4 \rightarrow DF + C_2D_3$ [4a], DF was detectable only in its highest energetically accessible vibrational state (v=4) owing to kinematic constraints and the authors concluded that the reaction occured through the direct abstraction of D by F. The DF angular distribution from that experiment, however, shows a marked forward-backward symmetry, indicating that the reaction may very well proceed through formation of a long-lived adduct followed by DF elimination. In a related experiment, Moehlmann and McDonald [35] found that the HF vibrational state distribution

from the reaction, $F + C_2H_4 \rightarrow HF + C_2H_3$, peaks at v=1. Radiative decay of HF in higher vibrational states before detection is, however, a possibility in that experiment. Donaldson et al. [36] observed an inverted HF vibrational distribution for the same reaction, which they take as support of a direct abstraction mechanism. However, it is also possible that an inverted HF vibrational state distribution can result from concerted HF elimination from a long-lived adduct [37].

In halogenated ethanes and ethylenes, 3- and 4-center elimination reactions are known to have activation energies in the range of 60-80 kcal/mol [37-39]. The activation energy for elimination of HF from C_2H_3F is 80 kcal/mol; from C_2H_5F it is 60 kcal/mol [38a-c]. Ab initio calculations by Kato and Morokuma [39] indicate that the barrier to 3-center HF elimination from C_2H_3F is about 1 kcal/mol lower than the 4-center barrier. However, the magnitudes of the barriers to HX elimination from haloethyl radicals are unknown. The 4-center barrier in fluoroethyl radical might be expected to be closer in magnitude to that for C_2H_5F since the C-C and C-F stretching and C-C-F bending frequencies are predicted to be similar in the two species [10,37]. Chemical activation experiments suggest that the activation energies for 3-center HX elimination from haloethanes are slightly higher than those for 4-center elimination [38d,e]. In particular, 3-center elimination of HX from haloethanes is thought to be improbable in the absence of a second halogen atom on the primary carbon to stabilize the

carbene product [38d,40]. However, the possibility of partial double bond formation during 3-center elimination of HF from fluoroethyl radical might lower the barrier to this process below 50 kcal/mol. The maximum energy available to the radicals in our experiment is ≈49 kcal/mol (E_c=2.5 kcal/mol).

In calculating the ratio of the RRKM constants, vibrational frequencies and moments of inertia for the radical and for the $H-C_2H_3F$ transition state were obtained from Kato and Morokuma [10]; frequencies for the $F-C_2H_4$ TS, the depth of the radical well relative to reactants (46 kcal/mol), and the barrier to H elimination (41 kcal/mol) were obtained from refs. 18 and 19. The moments of inertia for the radical and for the H elimination TS were taken from ref. 10; those for the $F-C_2H_4$ TS state were calculated using the optimized transition state geometry of Schlegel [19]. Frequencies and moments of inertia for a 3-center $HF-C_2H_3$ TS were derived from the calculations of Kato and Morokuma on $C_2H_3F \rightarrow HF + C_2H_2$ [39]. Three additional frequencies corresponding to C-H stretching and bending were added (3400, 1400, 950 cm^{-1}) and the C-C stretching frequency in the H atom elimination TS state was used. The $F-C_2H_4$ TS was assumed to be at the same energy as reactants (i.e. no barrier to addition) and the barrier to 3-center elimination was initially taken to be 45 kcal/mol.

Microcanonical RRKM rate constants were calculated for all three processes [41]. The calculated excitation function is scaled to the experimental points (F^+/F_2^+ = 0.20) using a

weighted least-squares fit and is plotted in Fig. 12. It is obvious that the calculated curve barely declines with increasing energy. This is because the rate constant for H elimination is much larger than those for the other pathways. Lowering the barrier to HF elimination increases the rate constant for this process proportionately at both the low and high energies and so does not change the slope of the calculated curve. Raising the barrier to 47 kcal/mol so that radicals formed at the lowest experimental collision energy could not eliminate HF also does not appreciably affect the curve. Neither does excluding high frequency C-H stretching vibrations from the calculation. We conclude that, with the assumption that the cross section for complex formation is independent of collision energy, the observed excitation function cannot be modeled using statistical theory.

Since the fraction of energy in the fluoroethyl complex that is tied up in rotation, and thus unavailable to break bonds, increases very little in the collision energy range studied ($E_{rot}/E_{tot} \approx 1\%$ at E_c=0.8 kcal/mol and ≈4% at E_c=2.5 kcal/mol, using values for **L** calculated above and a moment of inertia of 58 amu·Å^2 [10]), the only alternative explanation for the decline in S_r with increasing collision energy is that the probability of forming the initial adduct decreases with increasing energy. In their classical trajectory calculations on $H + C_2H_4 \rightarrow C_2H_5$, Hase <u>et al.</u> [35] found that the addition cross section rises steadily from $E_c \simeq 4$ to 20 kcal/mol, levels

off around 30 kcal/mol and drops only when $E_c > 60$ kcal/mol. This result is not surprising considering that the potential energy barrier to H atom addition is 3.5 kcal/mol on the PES used in the calculation. The initial rise in cross section occurs because wider approach angles become energetically accessible at higher energies. For $E_c < 20$ kcal/mol, the addition cross section is lower when a PES with a more restricted range of approach geometries is used. The decrease in the excitation function at higher energies results from an increase in the fraction of unproductive collisions in which the incipient C-H bond either never reaches its equilibrium length or, having reached its equilibrium length, ruptures in less than one vibrational period.

Although the $F + C_2H_4$ potential energy surface probably allows for a wider range of reagent approach geometries than the $H + C_2H_4$ PES, we might still expect the cross section for the reaction $F + C_2H_4 \rightarrow C_2H_4F$ to display a positive energy dependence if there were an appreciable potential energy barrier to F atom addition. A very convincing explanation for the drop in S_r with increasing collision energy is that the $F\text{-}C_2H_4$ interaction is dominated by a barrier-less, long range attractive potential. Such an interaction, characteristic of radical association reactions, gives rise to a loose transition state [15]. The cross sections (rate constants) for many radical association reactions have been found to display a negative energy (temperature) dependence [15,42]. For example, a classical trajectory

study of the $H + CH_3 \rightarrow CH_4$ reaction indicates that the reaction cross section decreases by a factor of ≈1.7 from 0 to 2 kcal/mol [43]. Recent measurements on the kinetics of methyl radical recombination [44] suggest a drop of ≈25% in the high pressure rate constant for this reaction over the temperature range 296 - 577 K. This trend is explained by modern transition state theory which locates the transition state for reactions without a potential energy barrier at the intermolecular distance at which the density of states along the reaction coordinate is a minimum, $r^\dagger$ [42,45]. As the collision energy (or temperature) is raised, $r^\dagger$ decreases, causing the transition structure to become tighter, i.e., the relative motion of the collision partners at the critical configuration becomes more hindered. Alternatively, if, for certain favorable approach configurations, the transition state is located at the centrifugal barrier to the reaction (the intermolecular distance at which the attraction between the reacting species is exactly balanced their centrifugal repulsion), $r^\dagger$ will decrease with increasing energy [15,46]. In either case, a drop in the reaction cross section (rate constant) will accompany the decrease in $r^\dagger$. Our results are therefore consistent with an early, reactant like transition state for the $F + C_2H_4$ addition reaction. It is noteworthy that higher level <u>ab initio</u> calculations on this and related systems (see Section I) yield transition state properties that are consistent with our findings [18,21,22].

V. CONCLUSIONS

Our results show that if there is a barrier to F atom addition to ethylene it must be much less than 0.8 kcal/mol, in agreement with evidence that halogen atom addition to alkenes proceeds with little or no activation energy and with recent ab initio calculations. The observed decline in the relative cross section with increasing collision energy indicates that formation of fluoroethyl radical is not independent of collision energy and suggests that long range attractive forces give rise to a loose adduct transition state. The CM C_2H_3F product angular distributions that fit our data at E_c=1.4 and 1.1 kcal/mol are not consistent with those previously found for this reaction at E_c=2.0 kcal/mol and might reflect the increased importance of symmetric F atom attack at low collision energies.

ACKNOWLEDGEMENTS

We would like to thank William Hase, H. Bernhard Schlegel, Gil Nathanson, and Gary McClelland for helpful discussions and H. B. Schlegel for providing us with results prior to publication. This work was supported by the Director, Office of Energy Research, Chemical Sciences Division of the U. S. Department of Energy under Contract No. DE-AC03-76SF00098.

REFERENCES

1. N. Colebourne and R. J. Wolfgang, J. Chem. Phys. 38, 2782 (1963).
2. T. S. Smail, R. S. Iyer, and F. S. Rowland, J. Phys. Chem. 94, 1041 (1972).
3. G. V. Pukals'kaya, N. F. Chebotarev, V. B. Kolovskii, and S. Ya. Pashezhetskii, Kinet. Katal. 21, 1063 (1980).
4. (a) J. M. Parson and Y. T. Lee, J. Chem. Phys. 56, 4658 (1972); (b) J. M. Parson, K. Shobatake, Y. T. Lee, and S. A. Rice, Faraday Discuss. Chem. Soc. 55, 344 (1973); (c) J. M. Farrar and Y. T. Lee, J. Chem. Phys. 65, 1414 (1976).
5. J. G. Moehlmann, J. T. Gleaves, J. W. Hudgens, and J. D. McDonald, J. Chem. Phys. 60, 4790 (1974).
6. R. A. Marcus, Faraday Discuss. Chem. Soc. 55, 379, 381 (1973).
7. R. A. Marcus, J. Chem. Phys. 62, 1372 (1975); G. Worry and R. A. Marcus, J. Chem. Phys. 67, 1636 (1977).
8. W. L. Hase and K. C. Bhalla, J. Chem. Phys. 75, 2807 (1981).
9. D. T. Clark, I. W. Scanlan, J. C. Walton, Chem. Phys. Lett. 55, 102 (1978).
10. S. Kato and K. Morokuma, J. Chem. Phys. 72, 206 (1980).
11. S. W. Benson and H. E. O'Neal, Kinetic Data on Gas Phase Unimolecular Reactions (NSRDS-NBS 21, US Dept. of Commerce, Washington, D. C., 1970).

12. J. A. Kerr and Parsonage, Evaluated Kinetic Data on Gas Phase Addition Reactions (CRC, Cleveland, 1972).

13. J. A. Kerr and A. C. Lloyd, Quart. Rev. 22, 549 (1968).

14. V. Bonacic-Koutecky, J. Koutecky, and L. Salem, J. Am. Chem. Soc. 99, 842 (1977) .

15. S. W. Benson, Thermochemical Kinetics (Wiley, New York, 2nd ed., 1976).

16. J. M. Tedder and J. C. Walton, Accts. Chem. Res. 9, 183 (1976); J. M. Tedder and J. C. Walton, in Fluorine Containing Free Radicals, ACS Symposium Series 66, J. W. Root, Editor (ACS, Washington, D. C., 1978) p. 107; D. C. Nonhebel and J. C. Walton, Free Radical Chemistry (Cambridge University Press, Cambridge, 1974).

17. J. M. Tedder and J. C. Walton, Trans. Faraday Soc. 62, 1859 (1966).

18. H. B. Schlegel, K. C. Bhalla, and W. L. Hase, J. Phys. Chem. 86, 4883 (1980).

19. H. B. Schlegel, J. Phys. Chem. 86, 4878 (1982).

20. C. Sosa and H. B. Schlegel, J. Am. Chem. Soc. 109, 4193 (1987).

21. H. B. Schlegel (private communication).

22. B. Engels and S. D. Peyerimhoff, J. Phys. Chem. 93, 4462 (1989). See also: B. Engels and S. D. Peyerimhoff, J. Mol. Struct. 138, 59 (1986).

23. (a) Y. T. Lee, J. D. McDonald, P. R. LeBreton, and D. R. Herschbach, Rev. Sci. Inst. 40, 1402 (1969); (b) R. K. Sparks, Ph. D. Thesis, University of California, Berkeley, 1979.

24. D. M. Neumark, A. M. Wodtke, G. N. Robinson, C. C. Hayden, and Y. T. Lee, J. Chem. Phys. 82, 3045 (1985); D. M. Neumark, Ph. D. Thesis, University of California, Berkeley, 1984.

25. R. J. Buss, Ph. D. Thesis, University of California, Berkeley, 1979.

26. Recently Jarvis and Grice have combined microcanonical RRKM theory with the theory of angular distributions from complex forming reactions to obtain a functional form for the product angular distributions arising from long-lived collision complexes that dissociate via oblate symmetric top transition states. They are able to reproduce reasonably well the C_2H_3F angular distributions obtained in ref. 4 by treating the fluorethyl radical as an oblate top. See, however, refs. 26 and 27. R. D. Jarvis and R. Grice, Mol. Phys. 66, 675 (1989).

27. G. M. McClelland and D. R. Herschbach, Faraday Discuss. Chem. Soc. 67, 251 (1979).

28. The moments of inertia of the C_2H_3F complex are given in ref. 10 as 13.2, 51.4, and 58.0 amu$\cdot$Å^2.

29. J. A. Shea and W. H. Flygare, J. Chem. Phys. 76, 4857 (1982).

30. W. L. Hase (private communication).

31. R. Behrens, Jr., A. Freedman, R. R. Herm, and T. P. Parr, J. Chem. Phys. 63, 4622 (1975).

32. P. Casavecchia, C. Becker, and Y. T. Lee (unpublished results).

33. C. W. Bock, P. George, and M. Trachtman, J. Mol. Spectrosc. 76, 191 (1979).

34. W. L. Hase, D. M. Ludlow, R. J. Wolf, and T. Schlick, J. Phys. Chem. 85, 958 (1981).

35. J. G. Moehlmann and J. D. McDonald, J. Chem. Phys. 62, 3061 (1975).

36. D. J. Donaldson, D. G. Watson, and J. J. Sloan, Chem. Phys. 68, 95 (1982).

37. S. Kato and K. Morokuma, J. Chem. Phys. 73, 3900 (1980).

38. (a) J. M. Simmie, W. J. Quiring, and E. Tschuikow-Roux, J. Phys. Chem. 74, 992 (1970); (b) P. Cadman, M. Day, A. W. Kirk, and A. F. Trotman Dickenson, J. Chem. Soc. Chem. Commun. 203 (1970); (c) P. Cadman, M. Day, A. F. Trotman-Dickenson, J. Chem. Soc. (A) 2498 (1970); (d) K. C. Kim, D. W. Setser, and B. E. Holmes, J. Phys. Chem. 77, 725 (1973); (e) K. C. Kim and D. W. Setser, J. Phys. Chem. 78, 2166 (1974).

39. S. Kato and K. Morokuma, J. Chem. Phys. 74, 6285 (1981).

40. (a) M. J. Perona, J. T. Bryant, and G. O. Pritchard, J. Am. Chem. Soc. 90, 4782 (1968); (b) K. C. Kim and D. W. Setser, J. Phys. Chem. 76, 283 (1972).

41. W. L. Hase and D. L. Bunker, Quantum Chemistry Program Exchange, University of Indiana, Bloomington, Indiana.

42. M. Quack and J. Troe, Ber. Bunseges. Phys. Chem. 81, 329 (1977).

43. R. J. Duchovic and W. L. Hase, J. Chem. Phys. 82, 3599 (1985).

44. M. T. Macpherson, M. J. Pilling, and M. J. C. Smith, J. Phys. Chem. 89, 2268 (1985).

45. (a) D. M. Wardlaw and R. A. Marcus, J. Phys. Chem. 90, 5383 (1986); (b) W. L. Hase, J. Chem. Phys. 64, 2442 (1976); (c) W. L. Hase, Chem. Phys. Lett. 139, 389 (1987).

46. S. W. Benson, Can. J. Chem. 61, 881 (1983).

Table 1. Experimental beam conditions.

E_c (kcal/mol)	C_2H_4 source temp. (°C)	C_2H_4 beam Speed ratio	v_{pk} (a (x10^4 cm/s) F	C_2H_4	$n_1n_2v_{rel}$ (arb. units)
0.8	-100 (neat)	5.7	4.3	6.5	0.011
1.1	-100 (neat)	*	6.1	6.5	0.086
1.4	30 (neat)	7.9	6.1	8.2	0.17
1.9	30 (neat)	*	8.7	8.2	0.77
2.0	30 (20% in He)	12.3	6.1	10.5	0.26
2.5	30 (20% in He)	*	8.7	10.5	1.00

(a): Peak laboratory velocity.

Table 2. Fraction of available energy in product translation and relative cross sections.

E_c (kcal/mol)	$\langle E'/E_{avl} \rangle$	S_r [a] (arb. units)
0.8	0.52	1.00 (.09)[b]
1.1	0.52	0.75 (.02)
1.4	0.51	0.72 (.01)
1.9	0.50	0.55
2.0	0.51	0.53 (.01)
2.5	0.51	0.45

(a): For $F^+/F_2^+ = 0.20$; numbers in parentheses are $\pm 1\sigma$ error bars arising from the uncertainty in the mean value of the normalization factor described in the text.

(b): $S_r(0.8)$ is an average of the relative cross sections obtained with an isotropic $T(\theta)$ and b(i) in Fig. 10; it is normalized to 1. The uncertainty in $S_r(0.8)$ arises, in part, from the uncertainty in $T(\theta)$.

FIGURE CAPTIONS

Fig. 1: Generalized reaction coordinate diagram for F + $C_2H_4 \rightarrow H + C_2H_3F$. Hatched region represents collision energy range.

Fig. 2: Kinematic ("Newton") diagram for F + $C_2H_4 \rightarrow H + C_2H_3F$ at E_c = 1.9 kcal/mol. $\mathbf{v}_{CM}$: Velocity of center-of-mass; θ_{CM}: Center-of-mass angle for the collision in LAB frame; $\mathbf{u}_{C2H3F}$: Maximum velocity of C_2H_3F product in center-of-mass frame; $\mathbf{v}_{L1}$ and $\mathbf{v}_{L2}$: slow and fast components of C_2H_3F velocity at angle θ in LAB frame. For a P(E') that peaks away from zero, these components will give rise to a bimodal TOF spectrum.

Fig. 3: C_2H_3F (m/e=46) laboratory angular distribution at E_c=2.5 kcal/mol; all of the data are shown. Fit obtained with T(θ) a(ii) in Fig. 10. Arrow indicates center-of-mass angle.

Fig. 4: C_2H_3F (m/e=46) laboratory angular distribution at E_c=2.0 kcal/mol; all of the data are shown. —— fit obtained with T(θ) a(i); ---- fit obtained with T(θ) a(ii).

Fig. 5: C_2H_3F (m/e=46) laboratory angular distribution at E_c=1.9 kcal/mol; all of the data are shown. ——— fit obtained with T(θ) b(i); ---- fit obtained with T(θ) b(ii).

Fig. 6: C_2H_3F (m/e=46) laboratory angular distribution at E_c=1.4 kcal/mol; all of the data are shown. ——— fit obtained with T(θ) c(i); ---- fit obtained with T(θ) c(ii).

Fig. 7: C_2H_3F (m/e=46) laboratory angular distribution at E_c=1.1 kcal/mol. Fits same as Fig. 6. Error bars represent 90% confidence limits.

Fig. 8: C_2H_3F (m/e=46) laboratory angular distribution at E_c=0.8 kcal/mol. — — — obtained with an isotropic T(θ); ---- obtained with T(θ) c(i); ——— obtained with T(θ) b(i). See Fig. 7.

Fig. 9: C_2H_3F (m/e=46) time-of-flight spectra at four collision energies. Solid lines are fits to data using P(E') distributions in Fig. 11. The following T(θ) distributions were used (see text): E_c=1.9, b(i); E_c=1.4 and 1.1, c(ii); E_c=0.8, isotropic.

Fig. 10: Center-of-mass frame C_2H_3F angular distributions used to fit laboratory angular distributions. (a), (b), and (c): [i] ——— ; [ii] -----.

Fig. 11: Center-of-mass frame product translational energy distributions used to fit the data at the six collision energies.

Fig. 12: Experimental excitation function for $F + C_2H_4 \rightarrow H + C_2H_3F$. Points are relative cross sections assuming $F^+/F_2^+ = 0.20$; see Table 2. Solid line is a RRKM calculation of the energy dependent branching ratio for this reaction (see text).

Fig. 13: Experimental excitation functions assuming different values for F^+/F_2^+.
□: $F^+/F_2^+=0.0$; ●: $F^+/F_2^+=0.20$; ○: $F^+/F_2^+=0.47$.

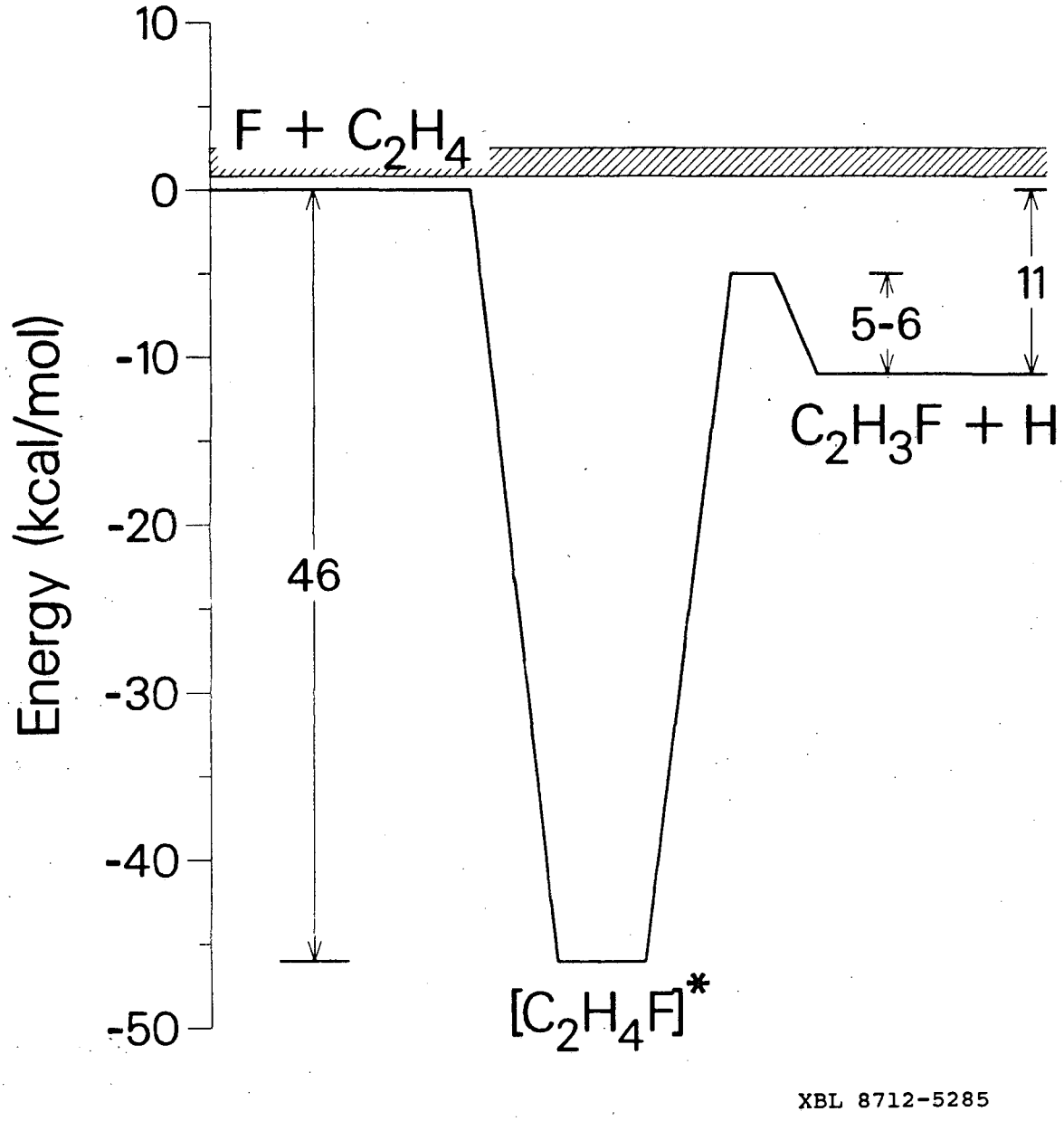
10
0
-10
-20
-30
-40
-50
Energy (kcal/mol)
F + C2H4
46
[C2H4F]*
5-6
11
C2H3F + H
XBL 8712-5285

Fig. 1

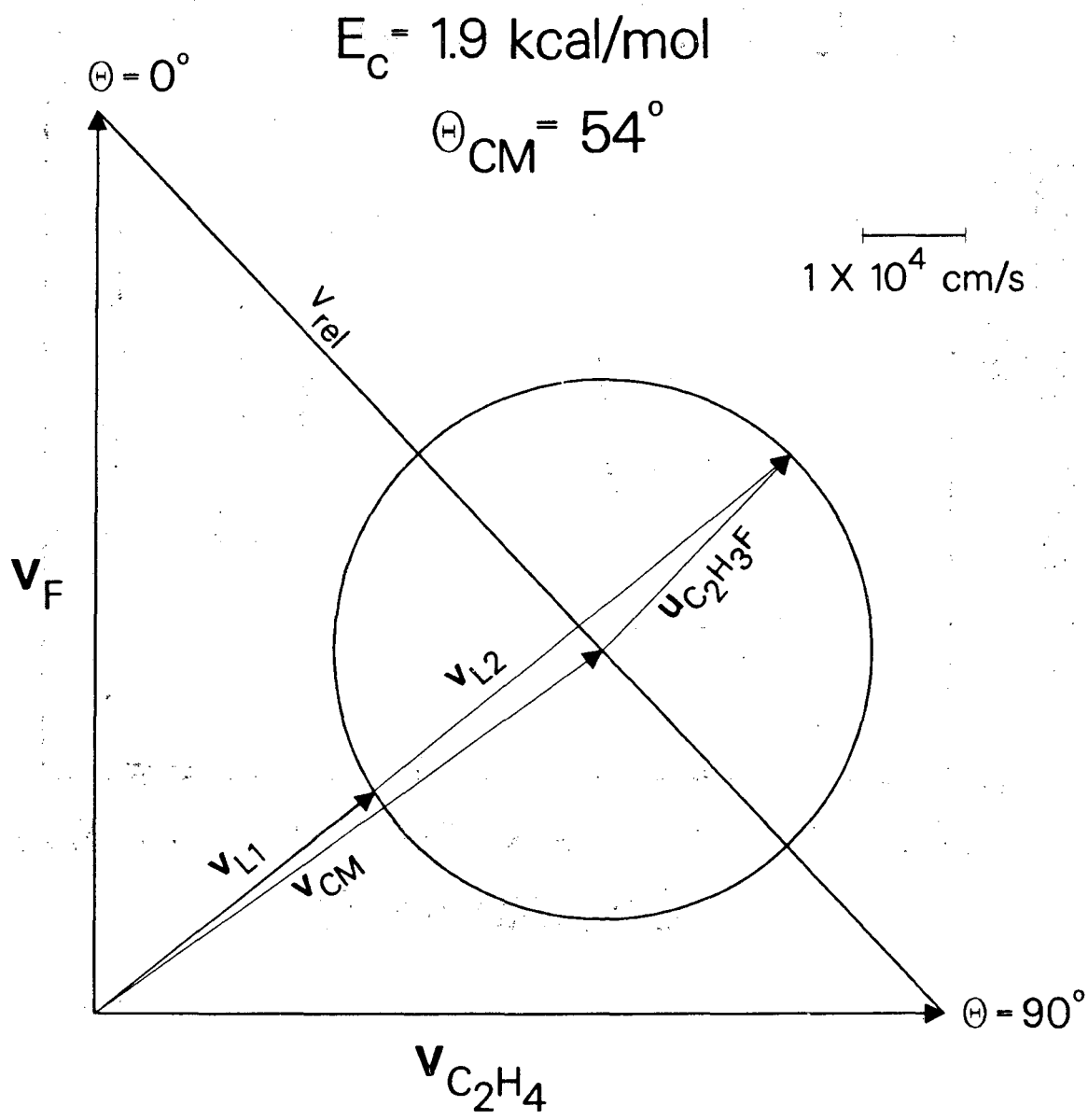

XBL 8712-5281

Fig. 2

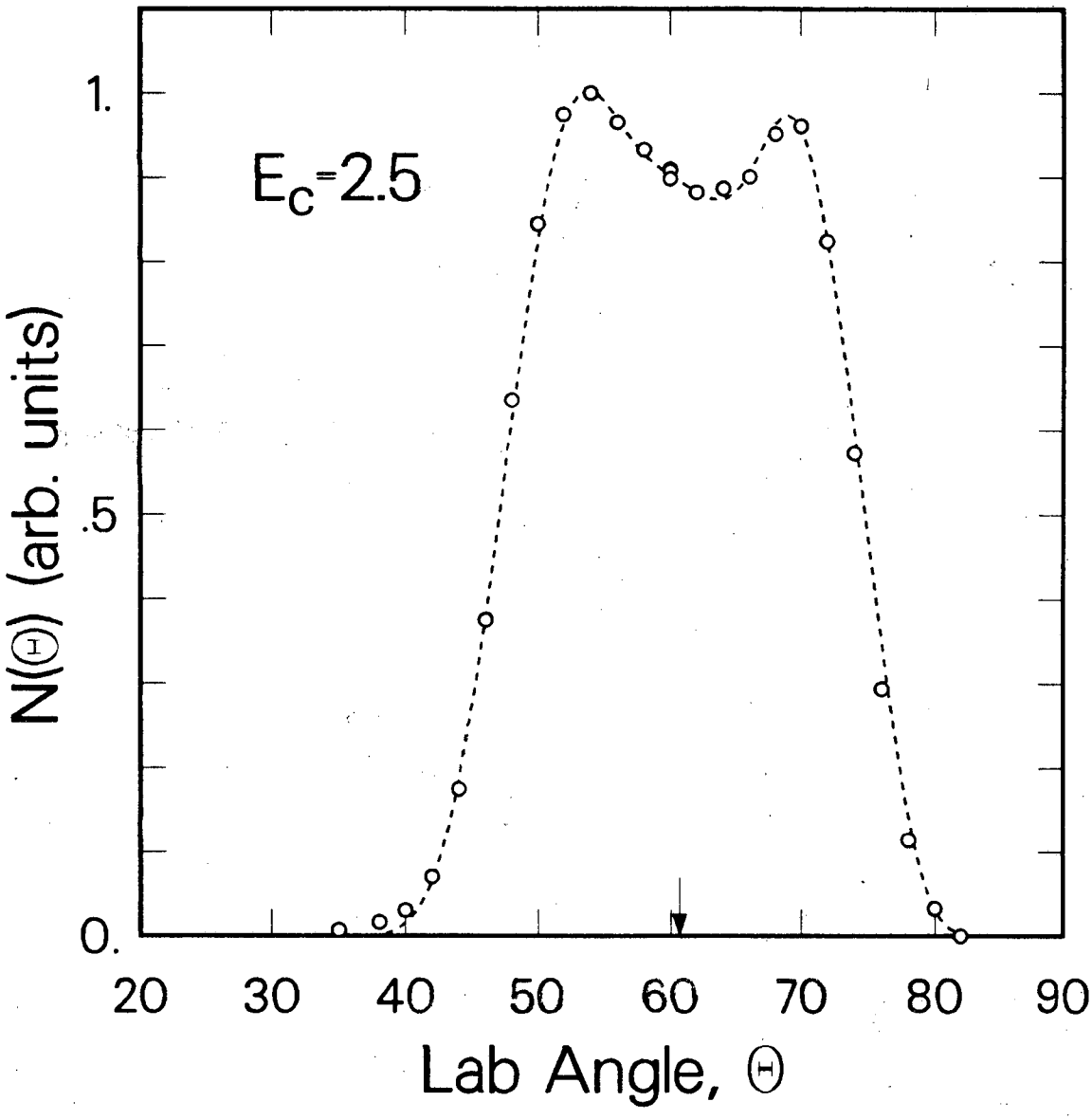

Fig. 3 XBL 8712-5329

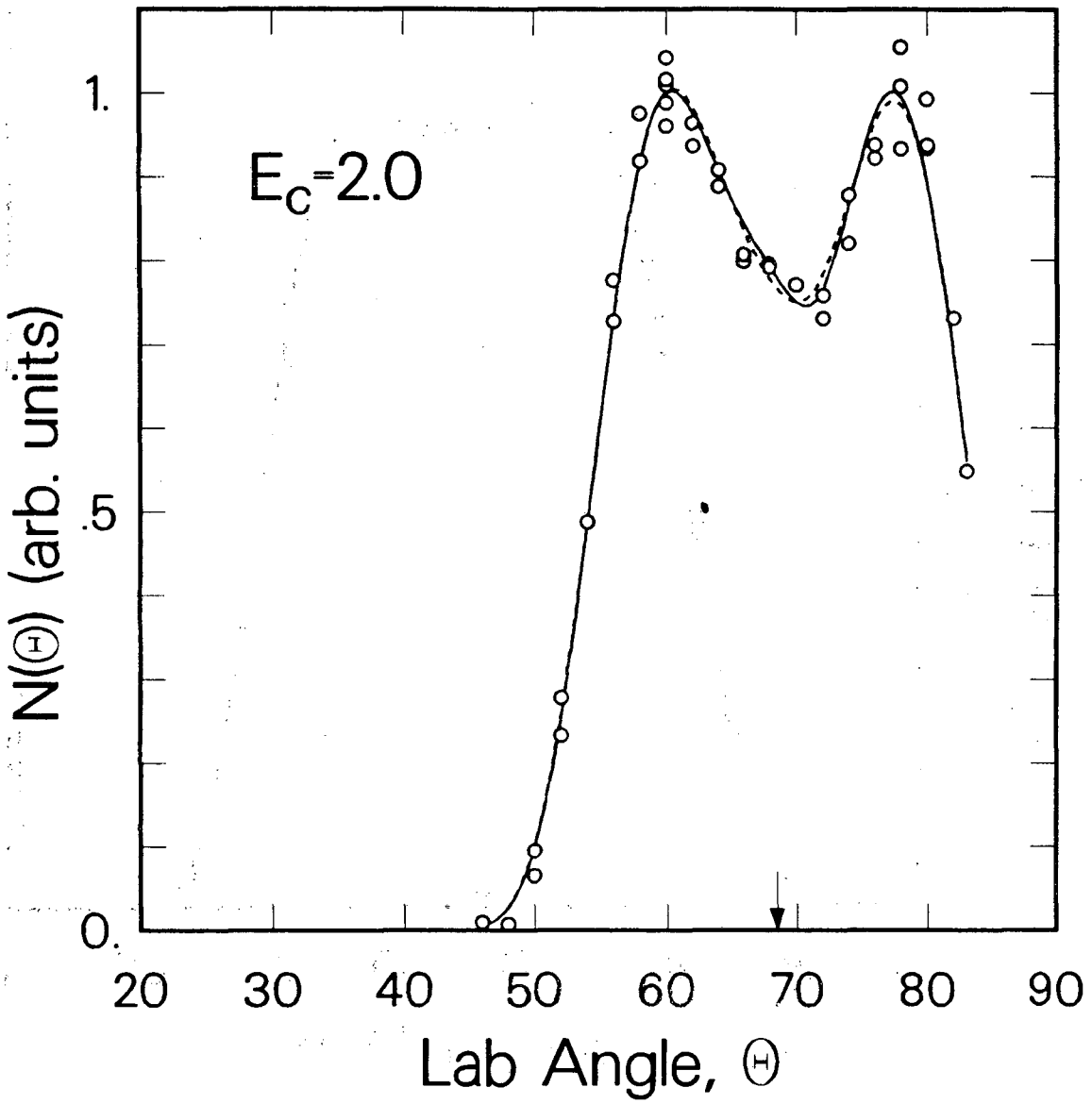

XBL 8712-5330

Fig. 4

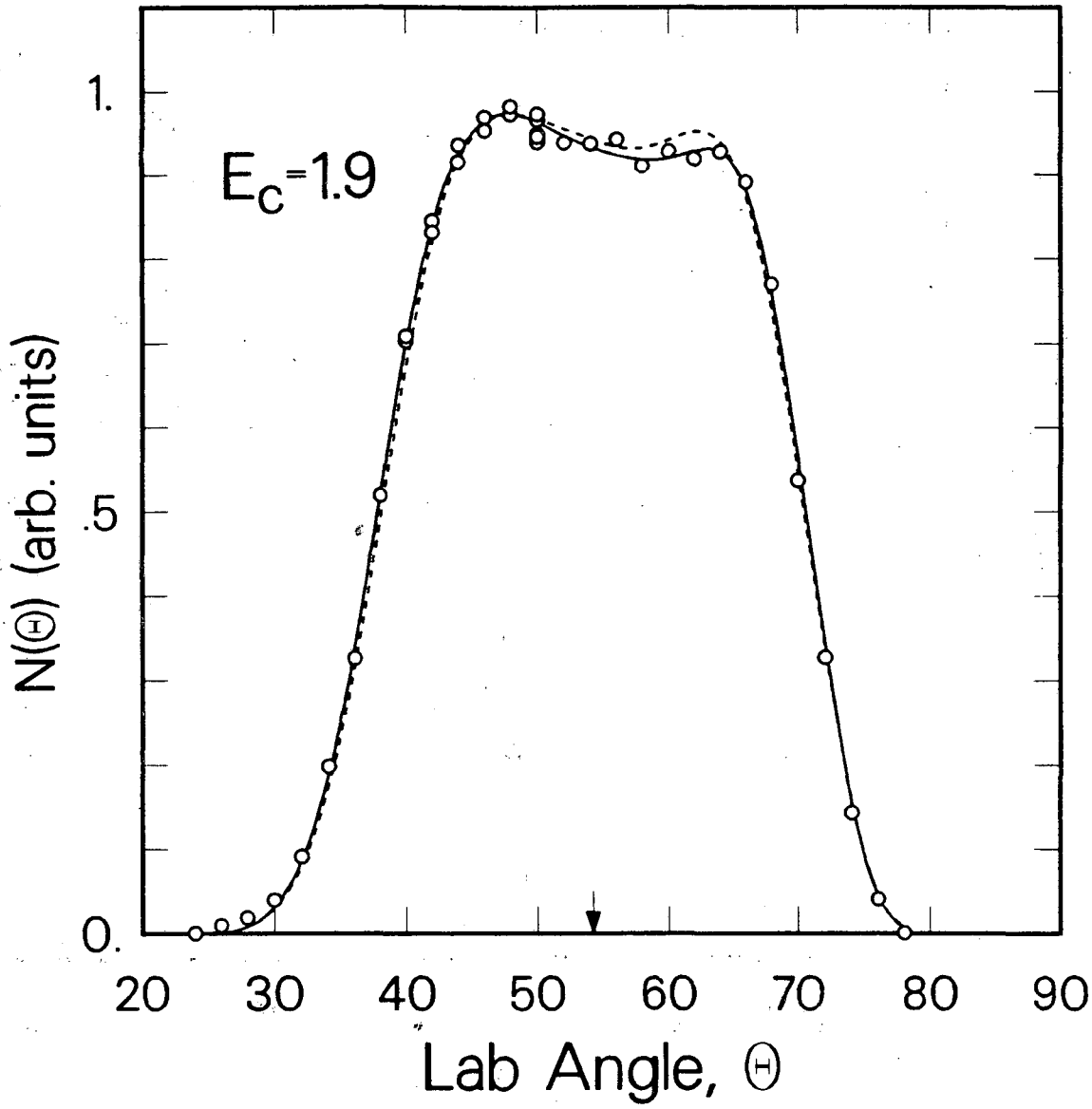

Fig. 5

XBL 8712-5324

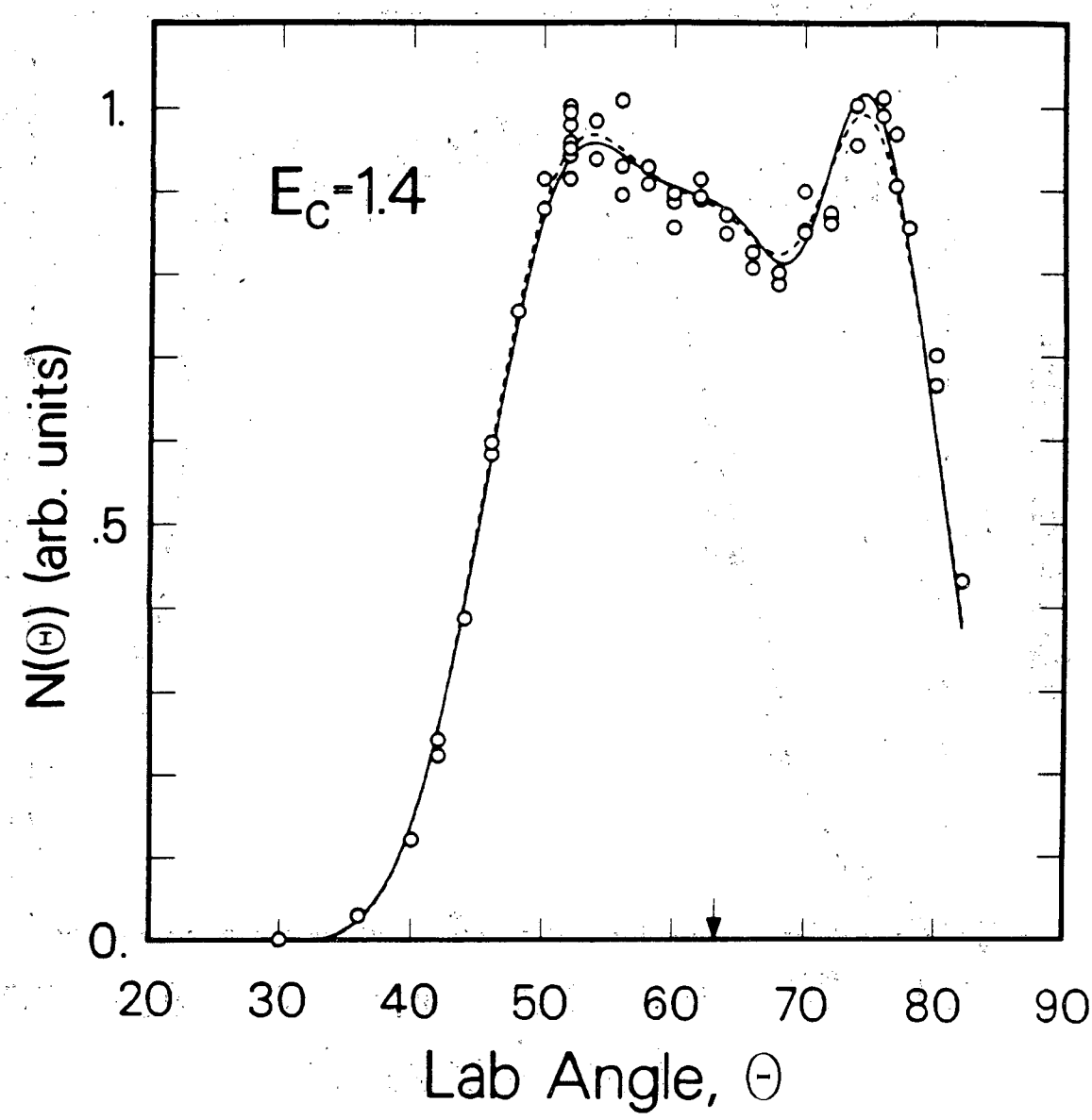

XBL 897-2797

Fig. 6

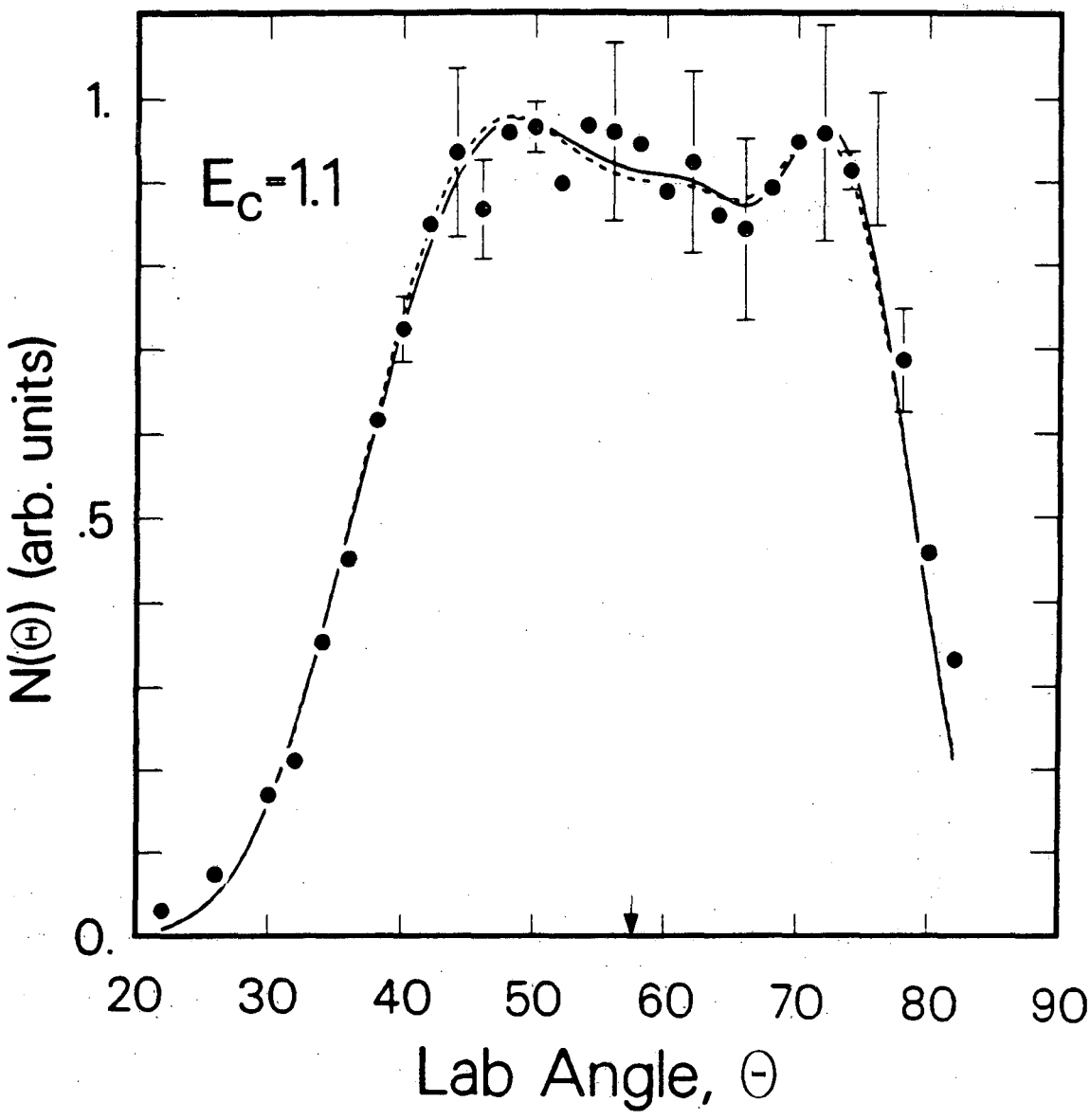

XBL 897-2796

Fig. 7

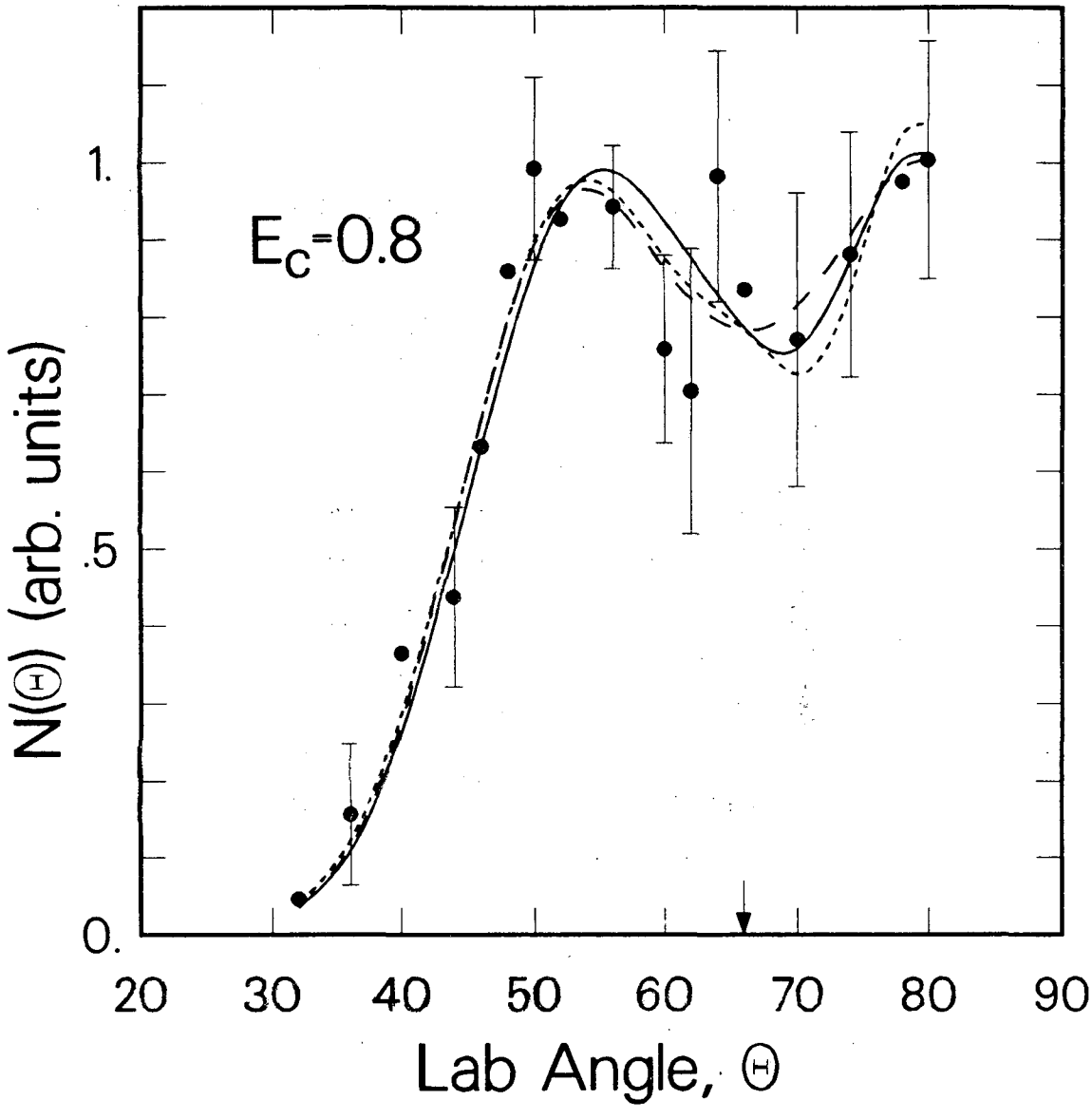

XBL 8712-5331

Fig. 8

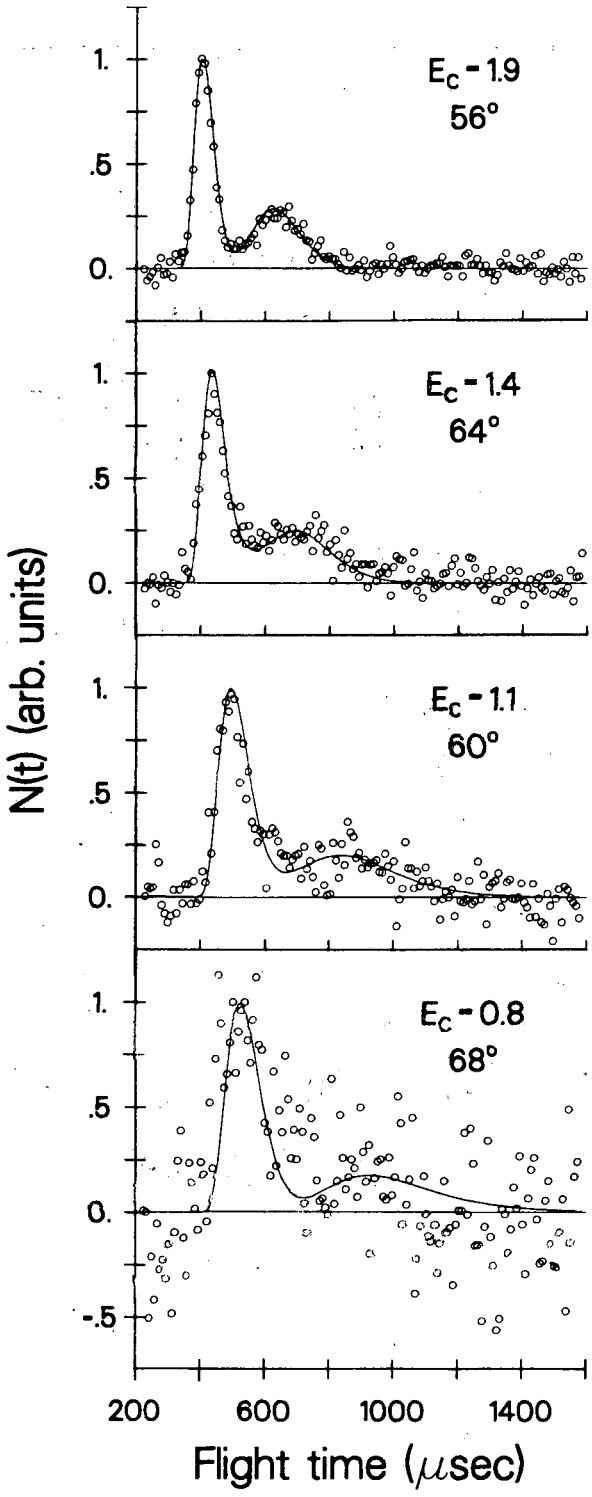

XBL 8712-5151

Fig. 9

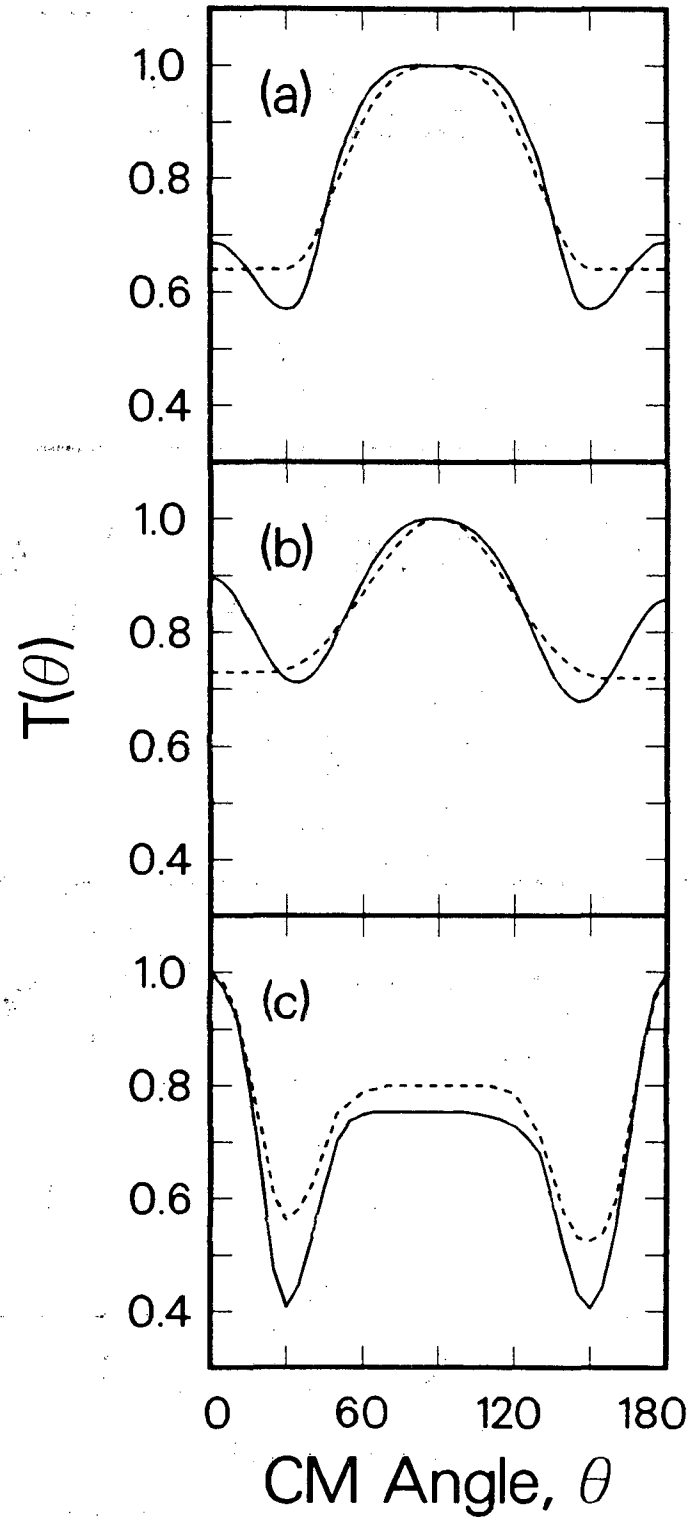

XBL 897-2798

Fig. 10

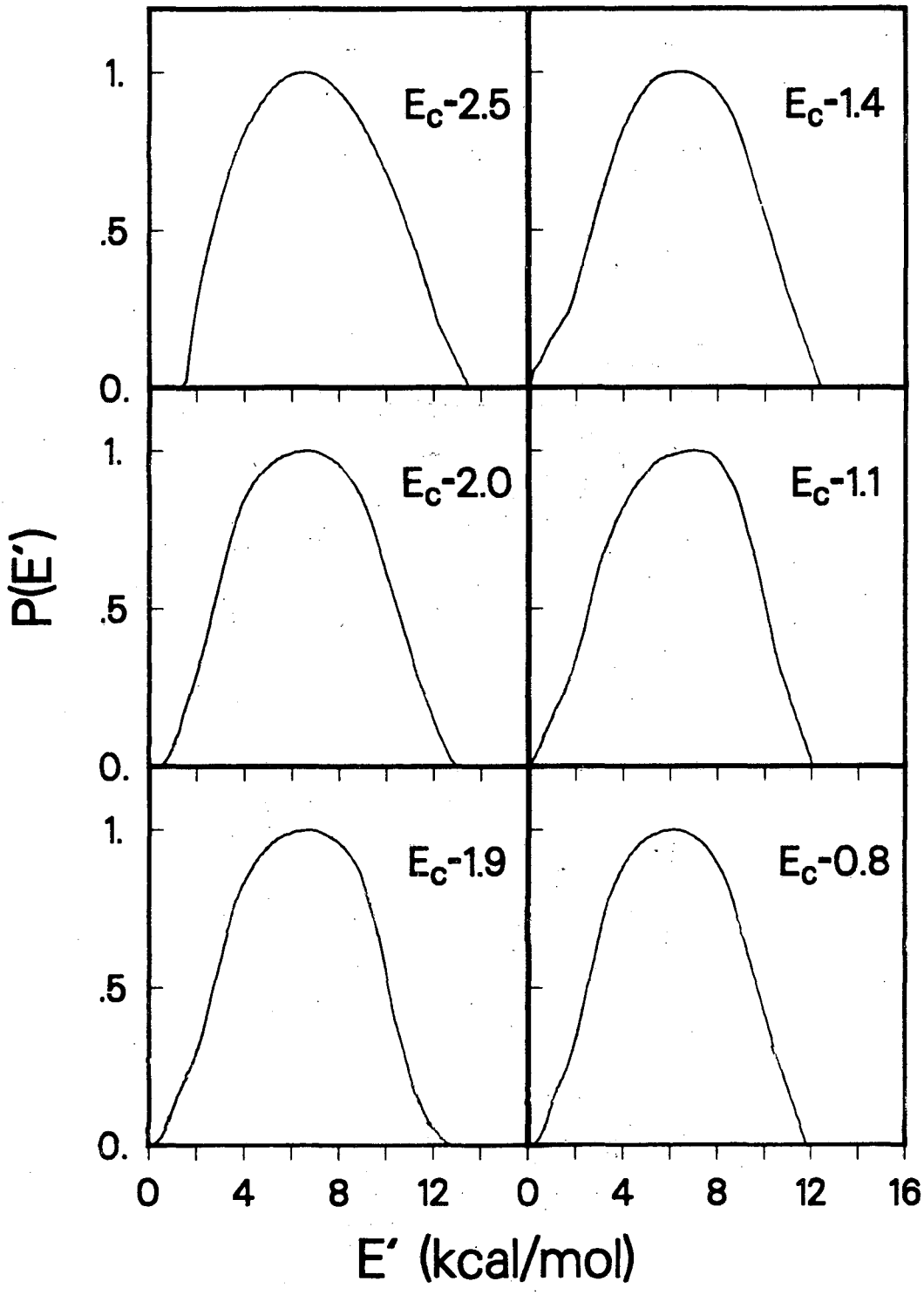

XBL 8712-5293

Fig. 11

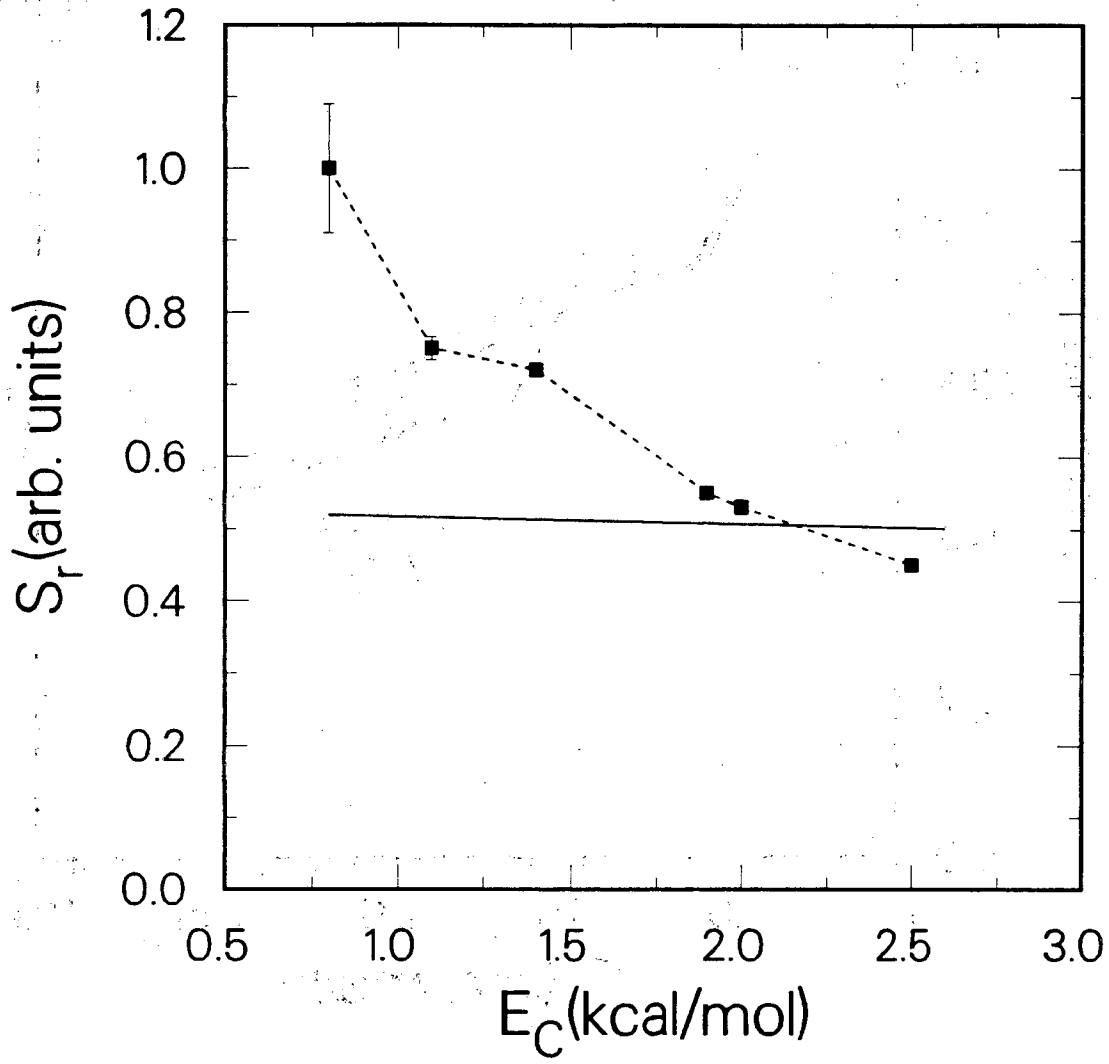

XBL 8712-5327

Fig. 12

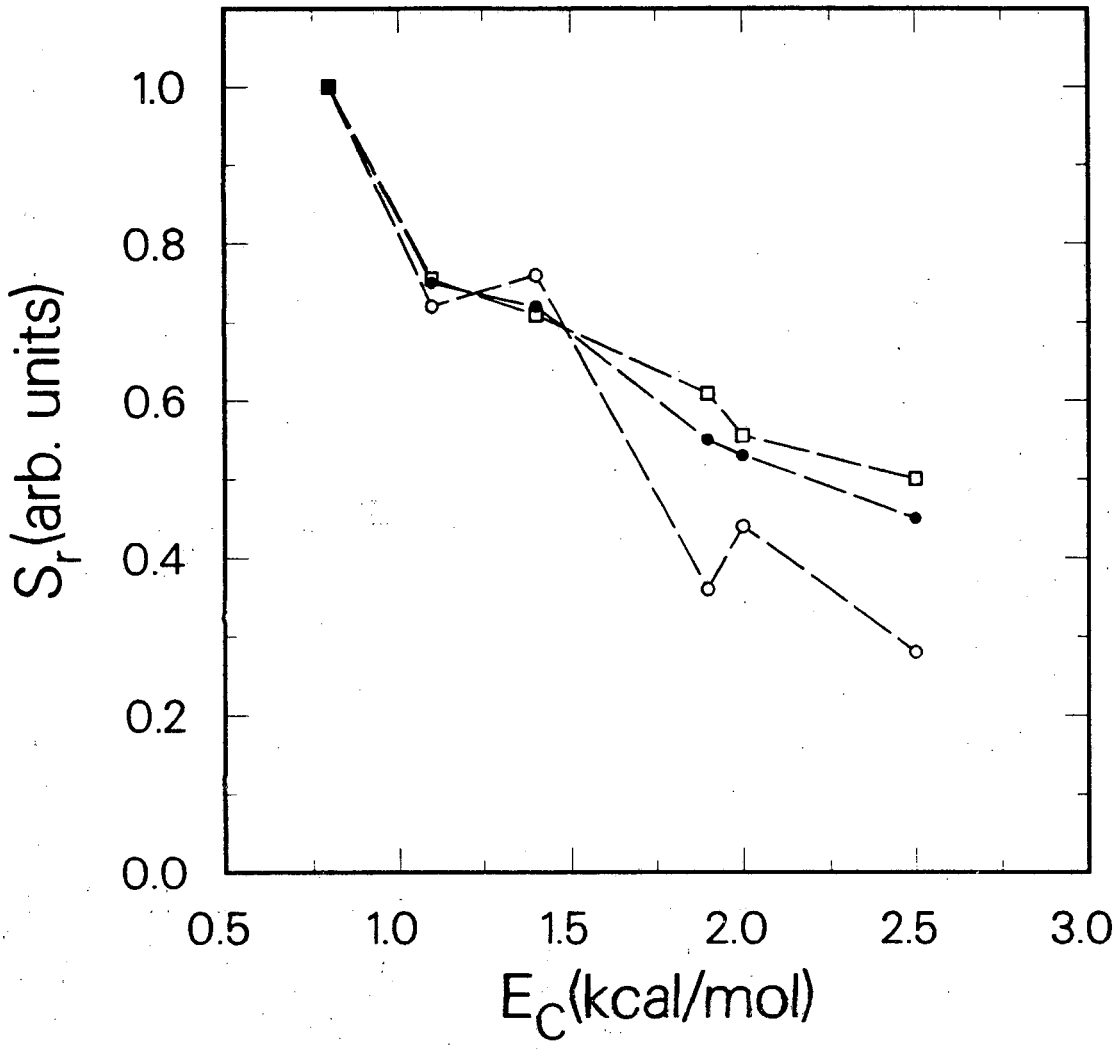

Fig. 13 XBL 8712-5326

LAWRENCE BERKELEY LABORATORY
TECHNICAL INFORMATION DEPARTMENT
1 CYCLOTRON ROAD
BERKELEY, CALIFORNIA 94720